AU J.T. 16(4): 206-214 (Apr. 2013)

Finite Element Analysis of Cardiovascular Stents

Chavdar Momchilov Hardalov, Mihail Stoyanov Mihalev [1], Plamen Petkov [2], Peter Stefanov [2] and Lilia Vladimirova-Mihaleva [3]

Department of Applied Physics, Technical University, Sofia, Bulgaria
E-mail: <chavdar_hardalov@tu-sofia.bg>

Abstract

The cardiovascular diseases have become contemporary and continuously growing healthcare problems. The main reasons for such problems are the intra-vessel depositions of plaque, cholesterol, etc., that give rise to thrombus formation, arterial blockage and stenosis. A traditional cure for said problems is to implant a stent. According to the "Guidance for Industry and FDA Staff - Non-Clinical Engineering Tests and Recommended Labeling for Intravascular Stents and Associated Delivery Systems", an intravascular stent is a tubular structure intended for permanent implant in native or graft vasculature. The stent is designed to provide mechanical radial support after deployment. This support is meant to enhance vessel patency over the life of the device. Once the stent reaches the intended location, it is expanded by a balloon or self-expanding mechanisms described below. There are two types of stents: the so-called balloon-expandable stents and self-expanding stents. The balloon-expandable stents are expanded by a catheter. They retain the required diameter after deflation of the catheter. The self-expandable stents are expanded from the pre-deployed to the post-deployed diameter size in absence of a catheter. This can be a result of the properties of the material or/and geometry. This work presents the finite element analysis (FEA) of mechanical behavior of balloon-expandable stents, produced from stainless steel 316L and Cobalt-Chromium alloy L-605.

Keywords: *Medical stents, fatigue, solid mechanics, finite element method (FEM), partial differential equation (PDE), computer-aided design* (*CAD*).

Introduction

The stents must support the vessels to hold the necessary blood flow. A stent is expanded by a balloon with a solution under pressure. The device retains a required diameter after the inflation of the balloon that is needed to hold the vessel wall. During this procedure, the mechanical properties and geometry of the stent change.

Recently, pre-clinical modeling and simulation of the mechanical behavior and fatigue lifetime of the deployed stents are becoming versatile tools.

The finite element analysis (FEA) is an excellent contemporary method for pre-clinical mechanical characterization. At present, there is a variety of software, based of FEA, for modeling of different physical processes with a high level of reliability.

Moreover, the simulations with a computer can be a good starting point for optimization of the stent design.

The increased usage of FEA for stent modeling led the Center for Devices and Radiological Health (CDRH) of the U.S. Department of Health and Human Services, Food and Drug Administration (FDA), to standardize this process in a document called "Guidance for Industry and FDA Staff - Non-

[1] Faculty of Mechanical Engineering, Technical University, Sofia, Bulgaria. E-mail: <mmihalev@tu-sofia.bg>.
[2] ISMA Ltd., Samokovsko Chaussee Str., 1138 Sofia, Bulgaria.
[3] Faculty of Physics, Sofia University, Sofia, Bulgaria. E-mail: <vladimirova@phys.uni-sofia.bg>.

Clinical Engineering Tests and Recommended Labeling for Intravascular Stents and Associated Delivery Systems". The most important parameters acquired from FEA are listed in Section IV B of the document and also explained below.

Percent surface area (PSA) is the ratio (in percent) of the partial area of the stent in contact with the vessel to the full area of the stent cylinder:

$$PSA = \frac{Area\,in\,contact\,with\,vessel}{Full\,cylindrical\,area} \times 100\%. \quad (1)$$

This area can affect the biological response of the vessel as described in Gosh *et al*. (2011) and Park *et al*. (2008).

Foreshortening is related to the final length of the stent after deployment. It can be used to estimate the proper stent length and placement in the blood vessel.

The foreshortening is defined as the ratio of the difference of final (loaded state) and initial (unloaded state) length, divided by the initial length:

$$F = \frac{L_{load} - L_{unload}}{L_{unload}} \times 100\%, \quad (2)$$

as described in Gosh *et al*. (2011) and Park *et al*. (2008).

Recoil of balloon expandable stent (RR) is related to the final stent diameter and delivers information about the proper choice of stent, acute post-implant results and clinical results.

The recoil, as described in Gosh *et al*. (2011) and Park *et al*. (2008), has been defined as:

$$RR = \frac{R_{load} - R_{unload}}{R_{unload}} \times 100\%, \quad (3)$$

where R_{load} and R_{unload} are the stent radii in post- and pre-inflated states, respectively.

Dogboning refers to the different expansion of the stent at distal ends and at the middle:

$$DB = \frac{R_{load}^{distal} - R_{load}^{central}}{R_{load}^{central}}, \quad (4)$$

as described in Gosh *et al*. (2011) and Park *et al*. (2008).

Fatigue analysis is needed because during the operation time the material properties change and failure due to fatigue is possible. In this case, the stent loses its function to support the vessel wall and a thrombosis formation or focal restenosis or (more dangerous) perforation of the wall are highly possible. Both are life-threatening states and the predictions of the device durability and lifetime are of highest importance (Stephens *et al*. 2001).

In compliance with CDRH (2010), a strain-based and a Goodman analysis are recommended. The fatigue safety factor can be estimated from Goodman diagram (Dowling 2004). The calculation procedure is described in the section Experimental Results of this work.

In addition, a stress-cycling analysis following the Smith-Watson-Topper algorithm (Stephens *et al*. 2001) has been performed, critical regions in the construction have been found and depicted, and the corresponding lifetime calculated.

Flexibility metric (FM) represents the bending moment of the curvature diagram and describes the flexibility of the stent:

$$FM = \int_0^{\chi_{\max}} M(\chi) d\chi, \quad (5)$$

where $M(\chi)$ is the bending moment and $\chi = \frac{2\phi}{L_{stentunit}}$ is the corresponding curvature of the stent unit being bent (Fig. 1) according to Petrini *et al*. (2004).

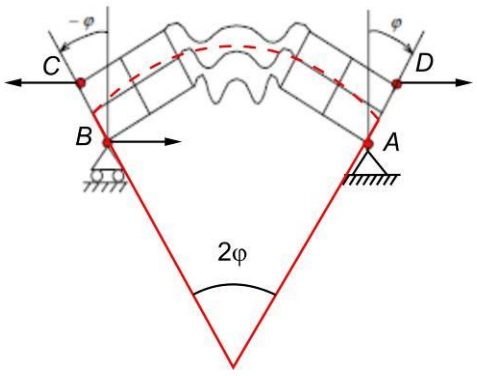

Fig. 1. Curvature diagram of a stent.

Experimental Results and Discussion

Geometrical Model

The design of a stent does begin with a choice of stent type and a repeated unit cell (RUC).

In this paper, a closed-shape stent, made of two types of materials (surgery steel 316L and Cobalt-Chromium alloy L-605), has been investigated. The RUC pattern is shown in Fig. 2. The struts that bind repeated cells have a width of 100 μm for 316L and 80 μm for L-605, respectively. The slight difference in the strut width is due to the specific mechanical properties of both materials.

A two-dimensional drawing of the unfolded cylindrical surface of the stent has been designed by applying translational and rotational operations of symmetry on the RUC (Fig. 3). The pattern has been repeated 5-fold along the longitudinal stent axis and 3-fold in perpendicular direction as shown in Fig. 3.

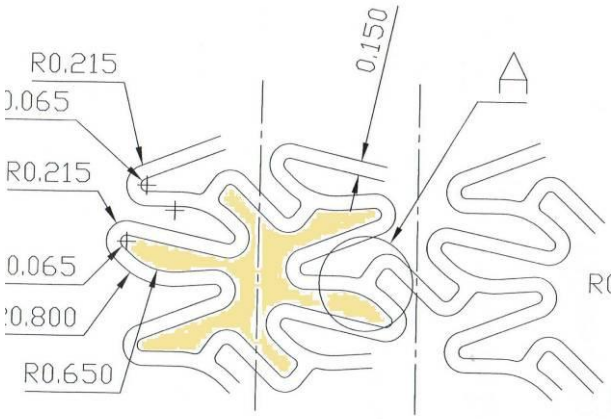

Fig. 2. RUC pattern.

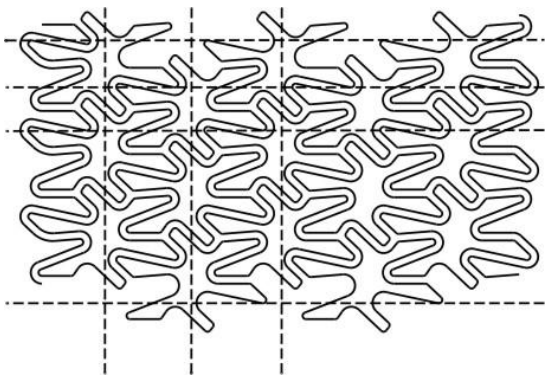

Fig. 3. Symmetry of the RUC.

Then the planar drawing has been imported into three-dimensional (3D) computer-aided design (CAD) software. From the pattern, a sheet of metal has been extruded with a thickness of the strut width. The sheet of metal has been folded into a tubular structure (Fig. 4). The 3D-geometry of the stent has been further imported into COMSOL® FEM-Software (COMSOL 2008).

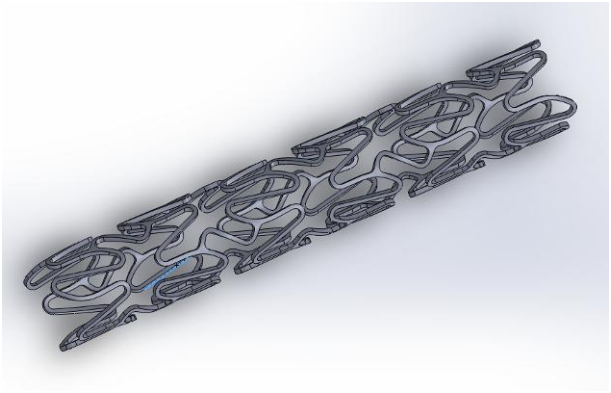

Fig. 4. Tubular structure.

Percent Area Surface (PSA)

The *PSA* has been calculated using the AutoCAD® internal module of region areas.

As a result, the values of *PSA* = 26% and *PSA* = 19.4% have been obtained for 316L and L-605 stents, respectively.

FE Analysis

A stationary solid mechanics model has been derived from Comsol® Solid Mechanics Module. The imported 3D-object has been meshed using internal COMSOL® mesh generator (COMSOL 2008). The balloon inflation causes plastic deformation of the stent. That is why, in addition to the elastic properties of the material (Young's modulus, Poisson's ratio), its inelastic properties must be defined in the elastoplastic section of the model.

A typical stress-strain curve of a material is shown in Fig. 5. At small strains (under 0.002), the mechanical behavior is described by the Hooke's law and a linearity between applied stress and occurred strain exists. The proportionality constant $E = d\sigma/d\varepsilon$ is called Young's modulus. This state is *reversible*, i.e. the body takes its previous form and dimensions (Stephens *et al*. 2001).

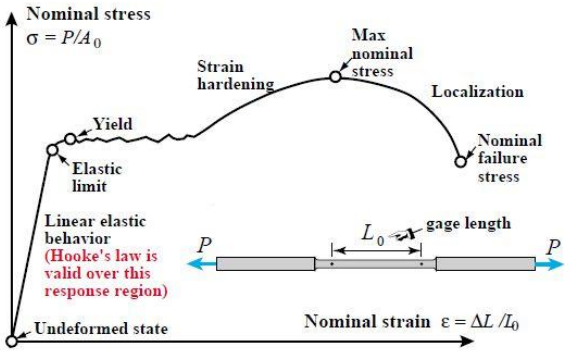

Fig. 5. Stress-strain curve.

The tensile strength, at which inelastic deformation occurs (ε = 0.002), is the *elastic limit* or *yield point* of the material. The inelastic deformations are irreversible (Stephens *et al*. 2001). The point, at which the sample is broken, is the *ultimate tensile strength* (Stephens *et al*. 2001).

Material constants (medical stainless steel 316L and Cobalt-Chromium alloy L-605) used in this work are listed in Table 1 (Gosh *et al*. 2011).

If a stress beyond the yield point is applied, the strain follows the stress-strain curve shown in Fig. 5. When the load is removed, the material returns to a state with zero stress in a path parallel to the elastic line (Fig. 6). In this case, a certain plastic deformation remains in the unloaded state (Stephens *et al*. 2001).

In the fully loaded state, the stent has a diameter limited by the balloon's diameter. After removing the balloon, the material is hardening and the stent deflates to a slightly reduced diameter due to the reasons, mentioned above.

The difference (in percent) between the stent diameters in fully loaded and fully relaxed states is called *recoil*. The diameter in the unloaded state must be equal to the diameter which is needed to guarantee the blood flow in the vessel. The big recoil of the stent is undesired because the stent must be over-inflated in order to reach the needed diameter. This can be dangerous, depending on the vessel's properties, as it can lead to injuries.

Table 1. Material constants (Gosh *et al*. 2011).

Parameter / Material	Young's modulus *E*, GPa	Yield stress σ_y, MPa	Ultimate Tensile Stress *UTS*, MPa	Poisson's ratio, unitless, ν
316L	198	200	610	0.3
L-605	243	630	1,100	0.297

Stent recoil calculations

In order to estimate the stent recoil, first a load has been applied to the inner surface of the struts that are in contact with the real balloon. The load does imitate the balloon inflation pressure. Because the balloon's inflation stops at practically selected diameters of 2, 3, 4 mm at pressure of most often 600 kPa, different boundary loads (550, 650 and 800 kPa for 316L and 800, 1,000 and 12,000 kPa for L-605) have been applied to achieve the desired deployment diameter (2, 3, 4 mm) of the stent.

The governing equation for solving the deformations of the stent during loading and unloading phases has the form:

$$\vec{\nabla} \bullet \hat{\sigma} = \vec{F}\,, \qquad (6)$$

where $\hat{\sigma}$ is the stress tensor and $\vec{F}$ is the force applied.

The boundary load has been given as force per unit area in opposite direction to the normal vector of the surface (Fig. 7, green surface).

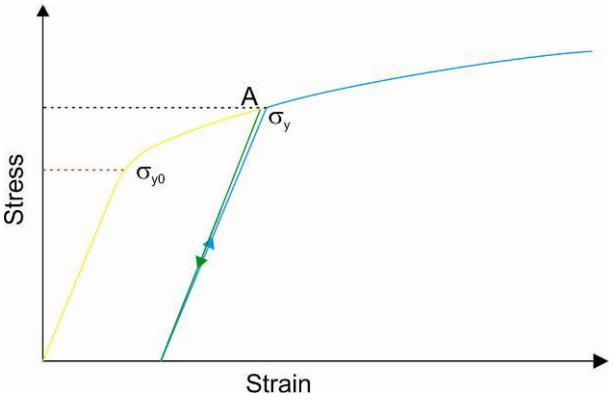

Fig. 6. Hardening of metal.

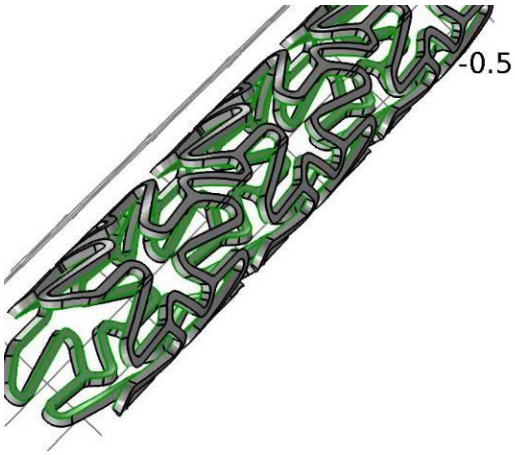

Fig. 7. Boundary load.

The rise of the inflation has been interpolated with a parameter *para* using the formula:

$$-Load*\left(para\left(para\le 1\right)+\left(2-para\right)\left(para>1\right)\right), \quad (7)$$

where *para* changes from zero to 2. The first part (*para* ≤ 1) represents the loading phase, and the second one (*para* > 1) - unloading.

The hardening phase can be calculated in two ways. The first one is to represent the stress-strain curve in the hardening region through an isotropic hardening function using the initial tangent at the yield point E_t as implemented in COMSOL (2008):

$$\sigma_{y_s}=\sigma_{y_{s0}}+\frac{E_t}{1-\frac{E_t}{E}}\varepsilon_{pe}. \quad (8)$$

This approach has been used for the 316L-stent. A value of $2x10^{10}$ Pa has been used for E_t taken from the literature (Gosh *et al.* 2011). In the case of the L-605 stent, the real tabulated stress-strain curve of the material obtained in the production process was used (Fig. 8, data from the supplier). This data has been imported into the COMSOL® software as an interpolation function.

Figure 9 shows the diameters of both stents in fully loaded and unloaded states as a function of the parameter *para* for a maximal balloon expanding size of 2 mm. The full process of inflation/deflation can be divided in three stages: 1) linear elastic stage (up to *para* = 0.5); 2) plastic deformation stage (0.5 < *para* < 1), when the yield point is reached; and 3) relaxation of the stent, when the load decreases to zero (*para* > 1).

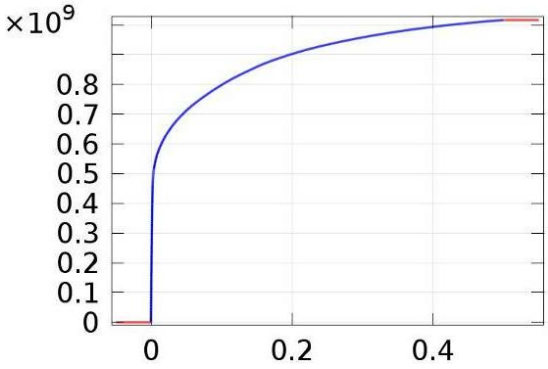

Fig. 8. Stress-strain curve (L-605 stent).

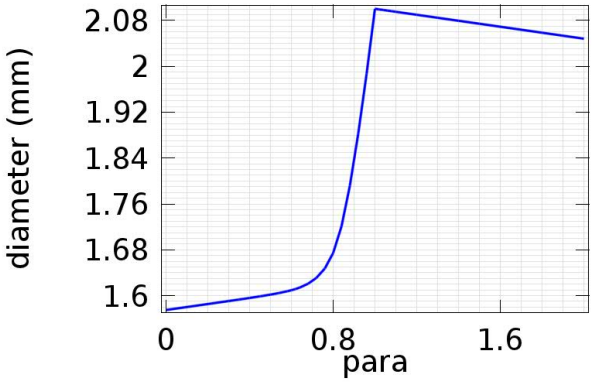

(a) 316L stent recoil.

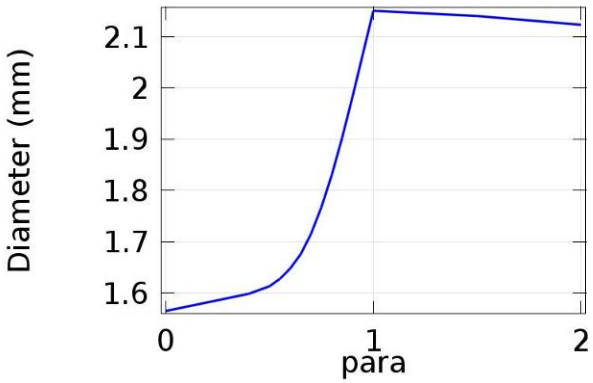

(b) L-605 stent recoil.

Fig. 9.Diameters of both stents as a function of the parameter *para*.

The plots show that the recoil of the stent made of stainless steel 316L is fully elastic (Fig. 9 (a)). The L-605 stent shows a slightly non-linear behavior (Fig. 9 ((b)).

Table 2 lists calculated averaged recoils of both stent types at different deployment diameters.

Table 2. Averaged recoils.

Parameter / Material	Recoil, %		
	2 mm	3 mm	4 mm
316L	3	1.80	1.85
L-605	5.8 (distal) 7.05 (cetral)		

It must be noted that the obtained recoils are in agreement with other authors (Gosh *et al*. 2011; Pochrząst *et al*. 2009). Real stent experiments with the RUC design, mentioned above, show a very good compliance with the results from the computer model.

Foreshortening

The linear deformations in loaded and exempt states have been observed with the graphical user interface (GUI). The result of the calculations is *FS* = 1.7% for the 316L stent. The foreshortening of L-605 has been found to be negligible.

Dogboning

For the stent construction, a dogboning of 1.7% has been found for the 316L stent having a deployment diameter of 2 mm and a length of 10 mm. The dogboning of L-605 has been found to be negligible.

Fatigue

The stent fatigue is a material failure due to a cyclic load. There are three phases: crack initiation, crack propagation and catastrophic overload failure (Marrey *et al*. 2006). The time appearance and duration of each of these phases depend on many factors such as material characteristics, magnitude of the stress and its orientation, and the preceding history (Stephens *et al*. 2001).

The failures can be studied as low-cycle and high-cycle fatigues. There is no strong sketched border between these types.

Low-cycle based fatigues are related to significant plastic deformations. Big cracks occur in the first cycle, but total destruction comes after a number of several, but relatively small, stress cycles.

Small plastic deformations, which are well localized, play a significant role in the *high-cycle* fatigue.

A straightforward way to predict the fatigue life is with the use of the so called *S-N* (stress - number of cycles) curve. A series of samples is tested for failure at different stresses. The *S-N* curve is the plot of crack stress versus number of cycles. The points lay along a line.

A better approach is to use the mean value at every stress range (Dowling 2004). The mean stress σ_m is the averaged value of the amplitude of cyclic loading, and the stress amplitude σ_a is the variation of this value (Fig. 10):

$$\sigma_a = \frac{\sigma_{\max} - \sigma_{\min}}{2}, \quad \sigma_m = \frac{\sigma_{\max} + \sigma_{\min}}{2}. \quad (9)$$

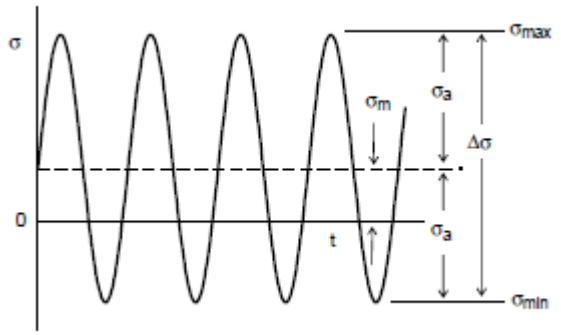

Fig. 10. Mean stress and stress amplitude.

By plotting the ratio σ_a/σ_m versus the mean stress, one receives a straight line, called a Goodman diagram (Fig. 11).

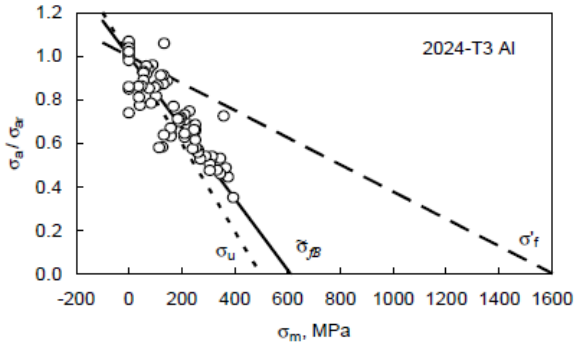

Fig. 11. Goodman diagram.

If the static pressure σ is equal to the ultimate tensile stress σ_u, the line corresponds to

$$\frac{\sigma_a}{\sigma} + \frac{\sigma_m}{\sigma_u} = 1. \quad (10)$$

This is the modified Goodman relationship. From the graph, it can be seen that all points below the dashed straight line cannot result in failures, i.e. this combination of mean and alternate stresses maintains safety.

In the case of a stent, a new load state (3) after the inflation (1) and relaxation (2) has been involved. Thus, the previous formula can be rewritten as follows:

$$\sigma_m = \frac{\sigma^3_{\max} + \sigma^2_{\min}}{2},\ \sigma_a = \left| \frac{\sigma^3_{\max} - \sigma^2_{\min}}{2} \right|. \qquad (11)$$

where $\sigma^3_{\max}$, $\sigma^2_{\max}$ the principal stress values.

Because the stress is a tensor quantity, it is consistent to take the second invariant of the stress deviation tensor, the von Mises stress for $\sigma^{2,3}{}_{\max}$ and $\sigma^{2,3}{}_{\min}$. The theory predicts that the yield or failure occur if the von Mises stress reaches a critical value for the chosen material.

By exporting the von Mises stresses and calculating the mean and alternate stresses, the points can be plotted in a σ_a-versus-σ_m diagram.

If all the points are located under the straight line, then, by drawing a parallel line over the point closest to the Goodman line, one can calculate the so-called *safety factor* (Fig. 12, a typical diagram for a 316L stent):

$$SF = \frac{\sigma_u}{\sigma_t}. \qquad (12)$$

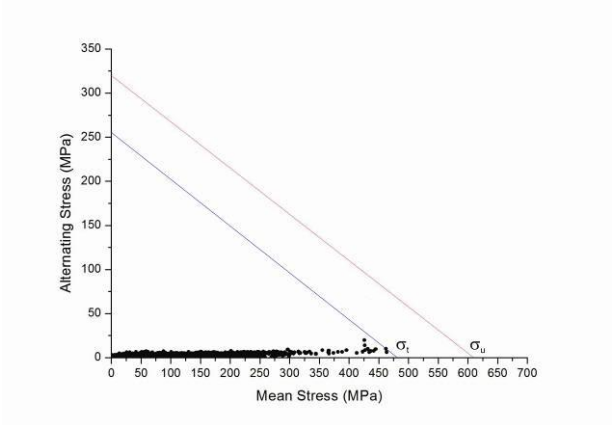

Fig. 12. Determination of the safety factor.

Table 3 lists the results of safety factor calculations for both stents.

Table 3. Safety factor calculations.

Parameter / Material	Safety factor		
	2 mm	3 mm	4 mm
316L	1.31	1.29	1.12
L-605	1.10	-	-

S-N fatigue analysis

For the S-N fatigue analysis, a new physics module has been added which implements the Smith-Watson-Topper (SWT) criterion for stress-cycling analysis (Stephens *et al*. 2001). The governing equation for the S-N analysis is:

$$\sigma_{\max} \cdot \frac{\Delta\varepsilon}{2} = \frac{\sigma'^2_f}{E} \times \left(2N_f\right)^{2b} + \sigma'^2_f \varepsilon'^2_f \times \left(2N_f\right)^{b+c}, \qquad (13)$$

where b, c, σ'^2_f and ε'^2_f are experimentally determined constants for each material.

The load has been applied using COMSOL® load groups, as required in S-N model. The load has been modulated by a cyclic pressure equal to the systolic blood pressure (80 mm Hg = 10.6 kPa) around the residual von Mises stress. The fatigue parameters used have been published by Benini (2010) and are shown in Table 4.

Table 4. Fatigue parameters (Benini (2010).

σ'_f , MPa	ε'_f	b	c
9.162	1.473	-0.14	-0.5

The results for the life cycles with the 316L and L-605 stents show a number of cycles approaching 10^8 in the worse case for both stents at a cyclic load of 80 mm Hg (10.6 kPa). This number of cycles is equal to the number of heart pulses for the duration of 10 years.

Flexibility analysis

The stent system is subjected to tight angulations during its delivery and exploitation in a blood vessel. If the flexibility of the stent is insufficient, either the struts could cause injury or the stent could fail. Therefore a new geometrical model has been created, consisting of only one single RUC. The RUC has been solidified by additional discs on both ends. The aim has been to prevent undesirable spurious deformations of the free ends of the struts. One point, acting as supporting point (point *A* in Fig. 1), has been fixed. The opposite point (point *B* in Fig. 1), acting as a roller, has been prevented to move perpendicular to the line *AB*. A force of 0.4 N directed to *A* has been exerted at *B*. Two pulling forces have been applied at points *C* and *D* with the same magnitude as in *B*. The whole system of forces delivers torques to both end plates of the RUC.

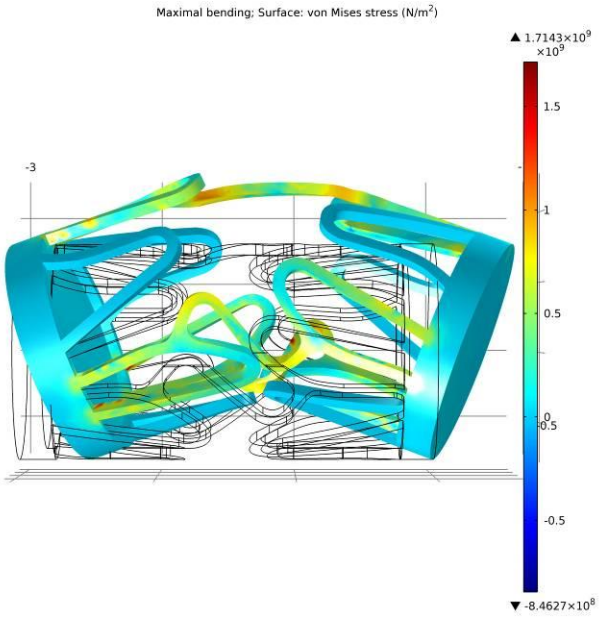

Fig. 13. Bending of RUC.

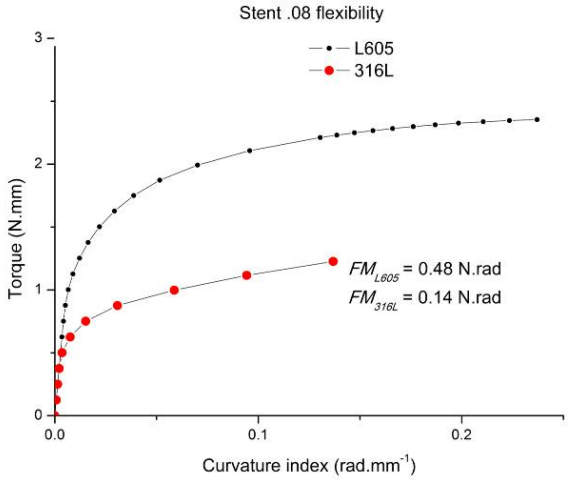

Fig. 14. Plot of torque $M(\chi)$ versus χ.

The result of bending is shown in Fig 13. The bending ends once the bottom binding struts contact. The curvature index χ of the stent being bent can be calculated from the geometrical analysis by following Petrini *et al.* (2004). The plot of the torque $M(\chi)$ versus χ is shown in Fig. 14. Calculations of the *FM* according to its definition (Eq. 5) give 0.48 N.rad for the L-605 stent and a lower value of 0.14 N.rad for the 316L stent.

Conclusion

In this work, a thorough analysis of two cardiovascular stents, being made from 315L stainless steel and L-605 Cobalt-Chromium (Co-Cr) alloy, has been performed in compliance with the recommendations of the "Guidance for Industry and FDA Staff - Non-Clinical Engineering Tests and Recommended Labeling for Intravascular Stents and Associated Delivery Systems" (CDRH 2010).

All procedures have been explained in detail and the obtained quantitative results have been presented in a comparative analysis between both stents. It has been shown that FEA is an appropriate and valuable tool for the prediction of the mechanical behavior and fatigue lifetime of the structures before production. All numerical results have been compared with the experimental structures in a pre-clinical study. Due to the substantial amount of technological and experimental information, the relevant technology scenarios and all experimental measurements have been omitted. A detailed comparison of the numerical results with the experiment will be published in a future work. The present study has been based on the comparative analysis between both stents only.

The stent made from L-605 shows bigger recoil than the stent made from 316L which is in favor of the latter due to the better ductility of the steel. Concerning other parameters, which depend to a higher extent on geometry and construction rather than on material properties, all of them are estimated as comparable.

The analysis of the critical stress parameters shows that during the inflation of the stent the von Mises stress in the Cobalt-Chromium stent is much lower than the critical values when compared to the similar stent, produced from 315L stainless steel.

Despite the nearly similar fatigue lifetime of both stents, a detailed analysis of the occurrences of possible cracks and their role for the fatigue would be a subject for further research in terms of material science.

Although both materials have similar mechanical behavior, the stainless steel stent reveals a better bending flexibility and, for that reason, the Cobalt-Chromium stents are produced with a thinner strut, independent from the common construction. The choice of material is based mainly on medical, biochemical and physiological considerations.

References

Benini, B.J. 2010. Tension and Flex Fatigue Behavior of Small Diameter Wires for Biomedical Applications. Master Thesis, Department of Materials Science and Engineering, Case Western Reserve University, Cleveland, OH, USA.

CDRH. 2010. Guidance for Industry and FDA Staff - Non-Clinical Engineering Tests and Recommended Labeling for Intravascular Stents and Associated Delivery Systems. U.S. Department of Health and Human Services, Food and Drug Administration (FDA), Center for Devices and Radiological Health (CDRH), Silver Spring, MD, USA.

COMSOL. 2008. Biomedical stent. COMSOL® Multiphysics version 3.5a - Documentation - Structural Mechanics Model Library. COMSOL, Inc., Burlington, MA, USA.

Dowling, N.E.; 2004. Mean stress effects in stress-life and strain-life fatigue. Proc. 2nd SAE Brazil International Conference on Fatigue: Fatigue 2004, São Paulo, Brazil, 21-23 June 2004. SAE Technical Paper No. 2004-01-2227, 14 pp. Society of Automotive Engineers (SAE), Warrendale, PA, USA.

Gosh, P.; DasGupta, K.; Nag, D.; and Chanda, A. 2011. Numerical study on mechanical properties of stents with different materials during stent deployment with balloon expansion. Proc. 2011 COMSOL Conference, Bangalore, India, 4-5 November 2011. 6 pp. Available: <http://www.comsol.pt/paper/download/84123/ghosh_paper.pdf>.

Marrey, R.V.; Burgermeister, R.; Grishaber, R.B.; and Ritchie, R.O. 2006. Fatigue and life prediction for cobalt-chromium stents: A fracture mechanics analysis. Biomaterials 27(9): 1988-2000.

Park, W.-P.; Cho, S.-K.; Ko, J.-Y.; Kristensson, A.; Al-Hassani, S.T.S.; Kim, H.-S.; and Lim, D. 2008. Evaluation of stent performances using FEA considering a realistic balloon expansion. World Academy of Science, Engineering and Technology, International Science Index 13, 2(1): 108-14. Available: <http://waset.org/publications/13128>.

Petrini, L.; Migliavacca, F.; Auricchio, F.; and Dubini, G. 2004. Numerical investigation of the intravascular coronary stent flexibility. Journal of Biomechanics 37(4): 495-501.

Pochrząst, M.; Walke, W.; and Kaczmarek, M. 2009. Biomechanical characterization of the balloon-expandable slotted tube stents. Journal of Achievements in Materials and Manufacturing Engineering 37(2): 340-7.

Stephens, R.I.; Fatemi, A.; Stephens, R.R.; and Fuchs, H.O. 2001. Metal Fatigue in Engineering. 2nd ed. John Wiley & Sons, Inc., New York, NY, USA.